# Compact Single Layer Travelling-Wave Antenna Design Using Metamaterial Transmission-Lines

Mohammad Alibakhshikenari [1]*, Bal Singh Virdee [2], and Ernesto Limiti [1]

[1] Electronics Engineering Department, University of Rome "Tor Vergata", Via del Politecnico 1, 00133 Rome – ITALY
[2] London Metropolitan University, Center for Communications Technology & Mathematics, School of Computing and Digital Media, London N7 8DB, UK
*[1]alibakhshikenari@ing.uniroma2.it, Phone number: +393886514777, [2]limiti@ing.uniroma2.it, [3]b.virdee@londonmet.ac.uk

***Abstract*— This paper presents a single-layer travelling-wave antenna (TWA) that is based on composite right/left-handed (CRLH)-metamaterial (MTM) transmission-line (TL) structure, which is implemented by using a combination of inter-digital capacitors and dual-spiral inductive slots. By embedding dual-spiral inductive slots inside the CRLH MTM-TL results in a compact TWA. Dimensions of the proposed CRLH MTM-TL TWA is 21.5×30.0 mm$^2$ or 0.372$\lambda_0$×0.520$\lambda_0$ at 5.2 GHz (center frequency). The fabricated TWA operates over 1.8–8.6 GHz with a fractional bandwidth greater than 120%, and it exhibits a peak gain and radiation efficiency of 4.2 dBi and 81%, respectively, at 5 GHz. By avoiding the use of lumped components, via-holes or defected ground structures (DGS), the proposed TWA design is economic for mass production as well as easy to integrate with wireless communication systems.**

***Keywords*—Travelling-wave antennas, planar antennas, microstrip, composite right/left-handed (CRLH), metamaterial transmission lines, inter-digital capacitor, double spiral inductor.**

## I. INTRODUCTION

Rapid development of next generation of wireless communication systems demands antenna designs that are compact, low profile and low-cost. The size of conventional antennas is too large for modern wireless systems especially at low frequencies. This necessitates the development of high performance compact antennas. Travelling-wave antennas (TWA) are a class of antennas that use a travelling wave on a guiding structure as the main radiating mechanism. These antennas offer good performance characteristics and have been widely employed in various microwave systems [1]. There are two categories of TWA, slow-wave antennas and fast-wave antennas, which are referred to as leaky-wave antennas. Slow-wave structures offer the potential for antenna size reduction. In slow-wave propagation the electric and magnetic energies are stored separately in the guided-wave media [2].

In recent years, the concept of composite right/left-handed (CRLH)-metamaterials (MTMs) has been extensively applied in the development of planar microstrip antennas [3]-[16], where miniaturization and good radiation characteristics have been reported. Design of such antennas however include the use of via-holes, defected ground structures or lumped elements, which are undesirable as these artifacts introduce additional complexity in the fabrication of the antenna and hence high cost, which limits their practical use [8], [9], [12], [13] and [14].

In this work, CRLH-MTM transmission-line is used to develop a compact travelling-wave antenna on a single-layer. CRLH MTM-TL is fabricated using inter-digital capacitors and dual-spiral inductive slots, where the slot is embedded in the transmission-line. The equivalent lumped element model of the CRLH MTM-TL is first analyzed. Both the simulated and measured results show good agreement with each other. The proposed TWA occupies an area of 21.5×30 mm$^2$, which is equivalent to 0.372$\lambda_0$×0.520$\lambda_0$, where $\lambda_0$ is free-space wavelength at 5.2 GHz. In addition, the proposed TWA avoids the use of via-holes, DGS, and lumped elements that is essential for low cost fabrication in mass production.

## II. MTM-TL BASED ON INTER-DIGITAL CAPACITORS AND DUAL-SPIRAL INDUCTIVE SLOTS

The CRLH-metamaterial transmission-line, shown in Fig. 1, is based on inter-digital capacitors and dual-spiral inductive slot elements. Unlike conventional CRLH metamaterial structures the symmetrical dual-spiral slot structure is embedded inside the 50Ω microstrip transmission-line with the series inter-digital capacitors located on either side of it. The proposed MTM-TL realized has compact dimensions.

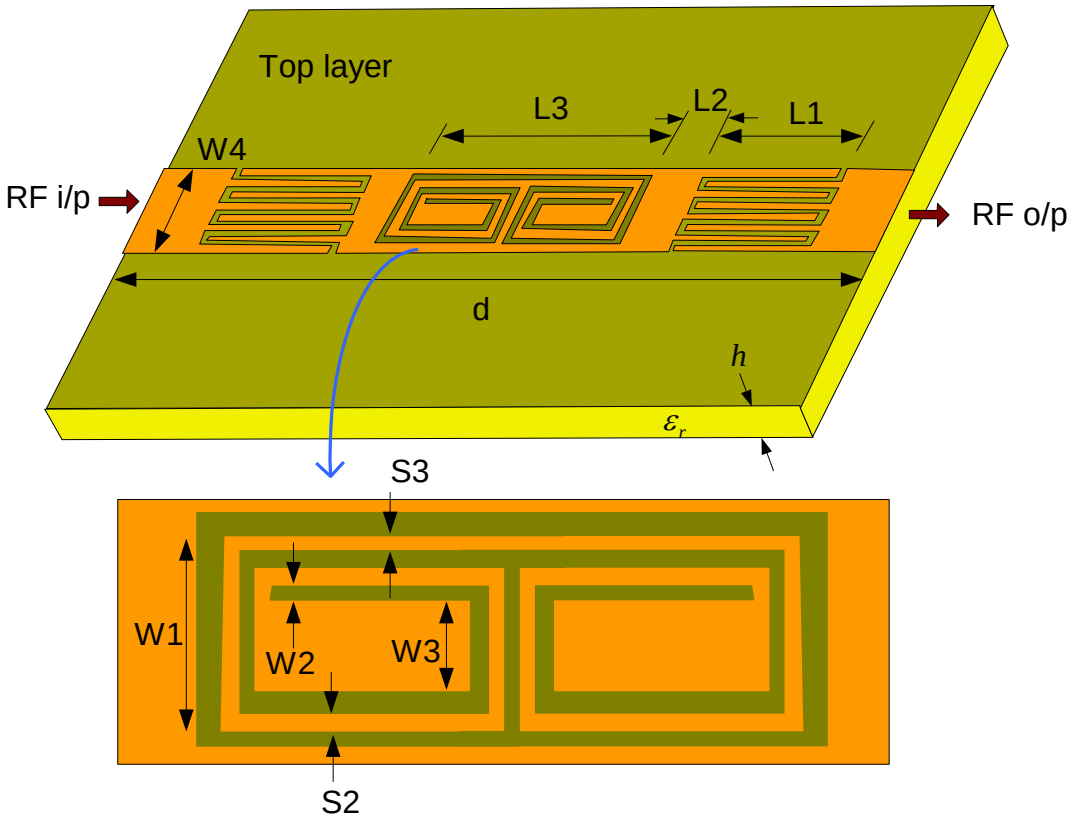


Fig. 1. Configuration of the proposed CRLH MTM-TL structure realized on 50Ω microstrip transmission-line.

The lossless lumped element equivalent circuit model of the proposed CRLH MTM-TL, shown in Fig. 2, is verified in [17], [18]. The lossless equivalent circuit model of the CRLH MTM-TL essentially resembles a T-type model, where $L$ represents for the transmission-line inductance, and $C_{inter.}$ represents the inter-digital capacitance. For accuracy, the model includes the fringing capacitance, $C_{fri.}$, associated with the inter-digital capacitors. The dual-spiral inductive slot is etched on the transmission-line, which is represented by the parallel resonant circuit comprising $C_{helix}$ and $L_{helix}$. The capacitance, $C_{coup.}$, accounts for the coupling between the transmission-line and the dual-spiral inductive slot structure.

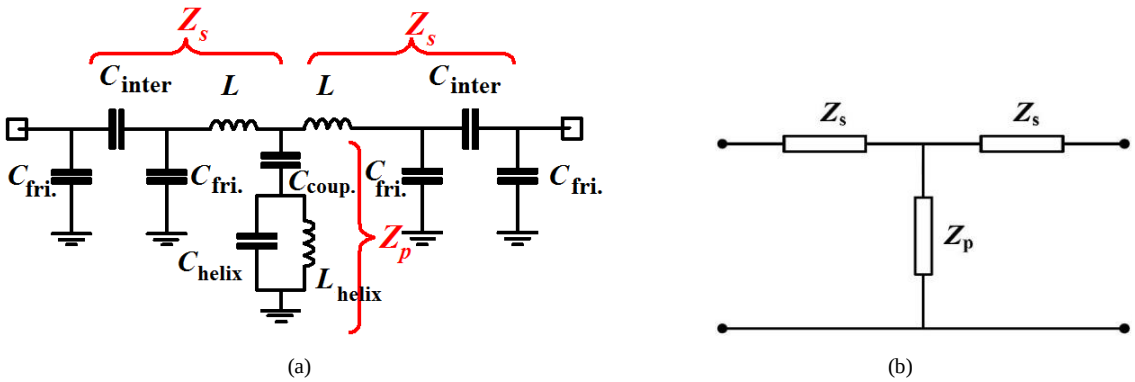


(a) (b)

Fig. 2. (a) The equivalent circuit model of proposed CRLH MTM-TL structure, and (b) generic T-type circuit model.

By applying the periodic boundary conditions related to the Bloch-Floquet theory, the dispersion relation, $\beta$, and the characteristic impedance, $Z_0$, of the proposed CRLH MTM-TL structure are given by [18]-[20]:

$$\varphi = \beta l = cos^{-1}[1 + Z_s(j\omega)Y_p(j\omega)] \qquad (1)$$

$$Z_0 = \sqrt{Z_s(j\omega)[Z_s(j\omega) + 2/Y_p(j\omega)]} \qquad (2)$$

Where, *l* is the length of the simplified lossless CRLH MTM-TL unit-cell in Fig. 2. As the fringe capacitance is negligible it is ignored in this analysis. The $Z_s(j\omega)$ and $Y_p(j\omega)$ represent the series impedance and shunt admittance, respectively, are given by:

$$Z_s(j\omega) = j\left[\omega L - \frac{1}{\omega C_{inter}}\right] \quad (3)$$

$$Y_p(j\omega) = j\frac{\omega C_{coup.}(\omega^2 L_{helix} C_{helix} - 1)}{[\omega^2 L_{helix}(C_{helix} + C_{coup}) - 1]} \quad (4)$$

From Eq. (4), a transmission zero is obtained by forcing the denominator to equate to zero, at:

$$f_z = \frac{1}{2\pi\sqrt{L_{helix}(C_{helix} + C_{coup})}} \quad (5)$$

It can be shown that the lower cutoff frequency, $f_s$, of the right-hand (RH) band and the upper cutoff frequency, $f_p$, of the left-hand (LH) band can be obtained by forcing $Z_s(j\omega)$ and $Y_p(j\omega)$ to be zero, hence:

$$f_s = \frac{1}{2\pi\sqrt{LC_{inter}}} \quad (6)$$

$$f_p = \frac{1}{2\pi}\sqrt{\frac{4C_{helix}}{4C_{helix}^2 L_{helix} + 5\, C_{coup} L_{helix} C_{helix}}} \quad (7)$$

Eqs. (6) and (7) are applicable on the assumption that $f_p < f_s$, and RH-band and LH-band transform as $f_p > f_s$. Under the balanced condition, namely $f_p = f_s$, there is no band-gap between the LH and the RH-bands [9].

The CRLH MTM-TL structure was constructed on Rogers RO4003 substrate with a relative dielectric constant of $\varepsilon_r$ = 3.38 and a thickness of $h$ = 0.8 mm. The frequency response of the proposed CRLH MTM-TL unit-cell, which is shown in Fig. 3, was obtained using Ansys's HFSS™ electromagnetic full-wave field solver, and the circuit model using Ansoft's Serenade™. Parameter extraction procedure involving the use of HFSS™ is described in detail in references [11] and [21], and considers complex S, Y, and Z parameters. The rigorous technique describes both the magnitude and the phase behavior of the waves travelling along the MTM-TL unit-cell structure. The physical dimensions of this structure are given in Table I.

Table I. Physical Dimensions of the Proposed CRLH MTM-TL Unit-Cell (units: mm)

| $W_1$ | $W_2$ | $W_3$ | $W_4$ | $d$ | $L_1$ | $L_2$ | $L_3$ | $S_1$ | $S_2$ | $S_3$ | $n$ |
|---|---|---|---|---|---|---|---|---|---|---|---|
| 3.0 | 0.2 | 0.65 | 3.5 | 27.5 | 5.7 | 1.5 | 9.0 | 0.18 | 0.2 | 0.2 | 10 |

There is good agreement between the HFSS™ and Serenade™. The dispersion diagram shows the velocity of phase is zero over 6 GHz to 6.8 GHz, which is the boundary of the LH and RH. It shows a phase lead over the passband from 2 GHz to 6.2 GHz, which confirms the MTM-TL behaves as a LH structure. A transmission zero at 2.1 GHz (lower than LH-band) provides a sharp transition. The dispersion relation and the characteristic impedance of the proposed CRLH MTM-TL were extracted from the scattering matrix. Tables II gives the values of the extracted equivalent circuit parameters for the MTM-TL unit-cell in Fig. 2(b). The frequency of the transmission zero, lower and upper cutoff frequency of the RH and LH were obtained by substituting the extracted parameter values in Eqs. (5) - (7). The calculated results agree well with simulation results which validates the theoretical model.

Table II. Extracted Circuit Parameters

| $C_{inter.}$ | $C_{fri.}$ | $C_{coup.}$ | $C_{helix}$ | $L_{helix}$ | $L$ |
|---|---|---|---|---|---|
| 0.41 pF | 0.13 pF | 0.75 pF | 4.38 pF | 0.50 nH | 3.56 nH |

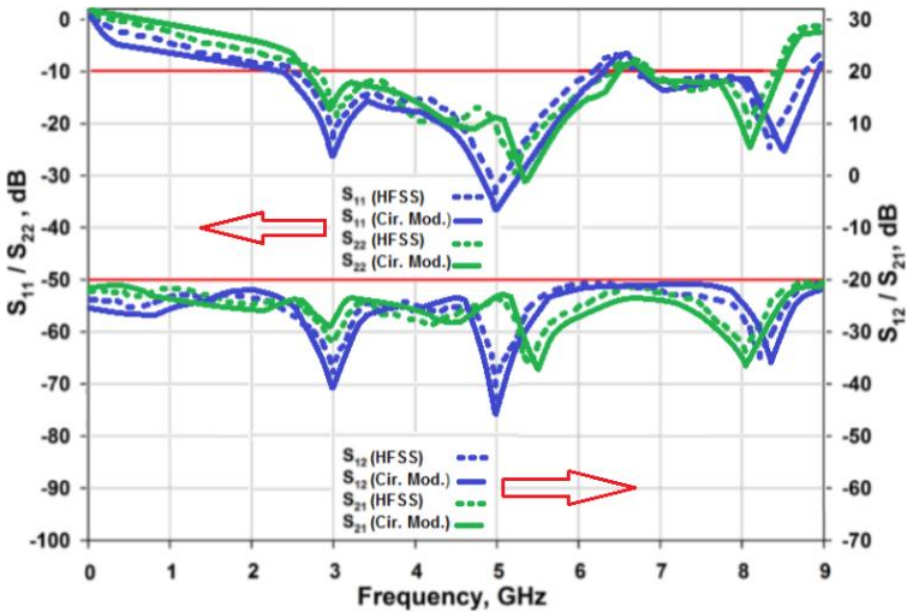


(a) Transmission and reflection-coefficient response (magnitude in dB)

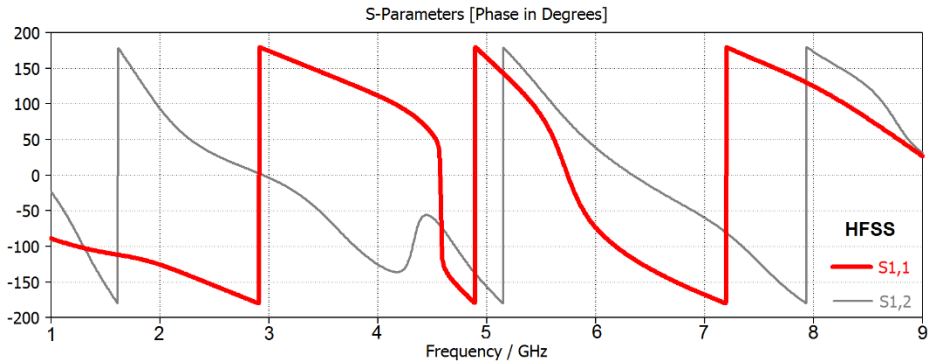


(b) Phase response (in degrees) of $S_{11}$ and $S_{12}$.

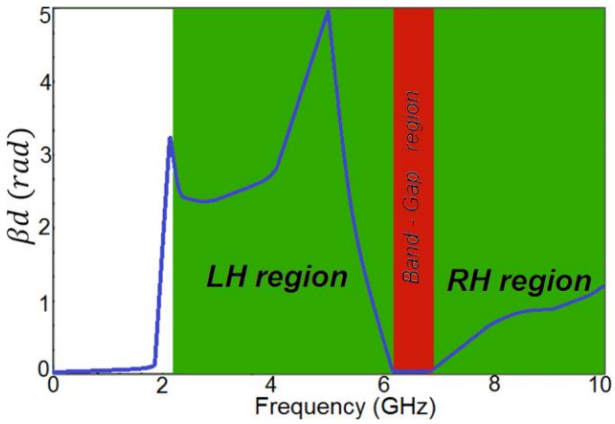


(c) Dispersion diagram

Fig. 3. (a) Transmission and reflection-coefficient response of the proposed CRLH MTM-TL structure, (b) Phase response, and (c) Dispersion diagram.

The CRLH MTM-TL was modeled as a two-port device in HFSS™. The S-parameters matrix of the CRLH MTM-TL was converted into its equivalent Z-parameters. The circuit model of the CRLH MTM-TL, shown in Fig. 2(b), is a T-type circuit. The following equations describe the relationship between S-parameters and Z-parameters for the T-type circuit:

$$Z_{11} = Z_{c1}\left[\frac{1-|S|+S_{11}-S_{22}}{|S|+1-S_{11}-S_{22}}\right] \quad (8)$$

$$Z_{12} = \sqrt{Z_{c1}Z_{c2}}\left[\frac{2S_{12}}{|S|+1-S_{11}-S_{22}}\right] \quad (9)$$

$$Z_{21} = \sqrt{Z_{c1}Z_{c2}}\left[\frac{2S_{21}}{|S|+1-S_{11}-S_{22}}\right] \quad (10)$$

$$Z_{22} = Z_{c2}\left[\frac{1-|S|-S_{11}+S_{22}}{|S|+1-S_{11}-S_{22}}\right] \quad (11)$$

Where, the termination port impedances $Z_{c1}$ and $Z_{c2}$ correspond to 50 Ω. As the proposed CRLH MTM-TL structure is a symmetrical, Eqs. (8) - (11) can be simplified to:

$$Z_{11} = Z_{22} = Z_{c1}\left[\frac{1-|S|}{|S|+1-2S_{11}}\right] \quad (12)$$

$$Z_{12} = Z_{21} = Z_{c1}\left[\frac{2S_{21}}{|S|+1-2S_{11}}\right] \quad (13)$$

The dispersion and characteristic impedance were calculated from Eqs. (1) and (2). The dispersion diagram in Fig. 3(b) shows the proposed CRLH MTM-TL creates a narrow band-gap between the LH and RH regions.

## III. Application of CRLH MTM-TL to the Proposed Travelling-Wave Antenna

### *A. Implementation of CRLH-MTM Unit-Cell on 75 Ω and 20 Ω Transmission-Lines*

To apply the proposed CRLH MTM-TL in the design of a travelling-wave antenna required the implementation of the CRLH-MTM unit-cell on 75 Ω and 20 Ω transmission-lines. Table III gives the geometrical parameters of the CRLH MTM-TL designed on 75 Ω and 20 Ω microstrip-lines. Parametric study of key parameters of the CRLH MTM-TL, i.e. $S_1$, $S_2$, $S_3$, $W_1$, $W_2$, $W_3$, and $W_4$, on the insertion-loss and return-loss response of the 75 Ω and 20 Ω MTM-TLs are shown in Fig. 4. Effect of these parameters on the CRLH MTM transmission line's performance is summarized in the Table IV. It is evident from the S-parameter response of both 75 Ω and 20 Ω CRLH MTM-TLs that by decreasing $S_1$ and $S_2$ and by increasing $S_3$ the performance of MTM-TLs improves over the desired range. The improvement also applies with modification of $W_1$, $W_2$, $W_3$, and $W_4$. The dimensions of the 75 Ω and 20 Ω CRLH MTM-TLs are 30×3.85 mm$^2$ and 21.5×5.3 mm$^2$, respectively, which corresponds to $0.180\lambda_0 \times 0.023\lambda_0$ and $0.129\lambda_0 \times 0.0.031\lambda_0$, respectively, at 1.8 GHz.

Table III. Structural Parameters for 75 Ω and 20 Ω CRLH MTM-TL (Units: mm)

| Parameters | 75 Ω | 20 Ω |
|---|---|---|
| $W_1$ | 3.50 | 5.15 |
| $W_2$ | 0.15 | 0.12 |
| $W_3$ | 0.90 | 1.10 |
| $W_4$ | 3.85 | 5.30 |
| $D$ | 30.0 | 21.5 |
| $L_1$ | 6.50 | 5.95 |
| $L_2$ | 1.40 | 1.40 |
| $L_3$ | 9.80 | 6.10 |
| $S_1$ | 0.12 | 0.12 |
| $S_2$ | 0.12 | 0.12 |
| $S_3$ | 0.12 | 0.12 |
| $N$ | 10 | 20 |

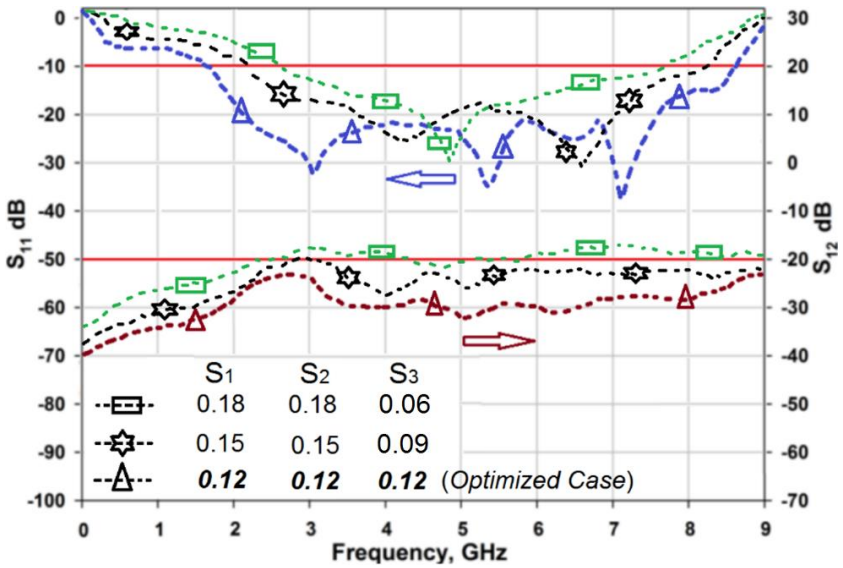


(a) 75 Ω (Dimensions of $S_1$, $S_2$, and $S_3$ are in millimeters)

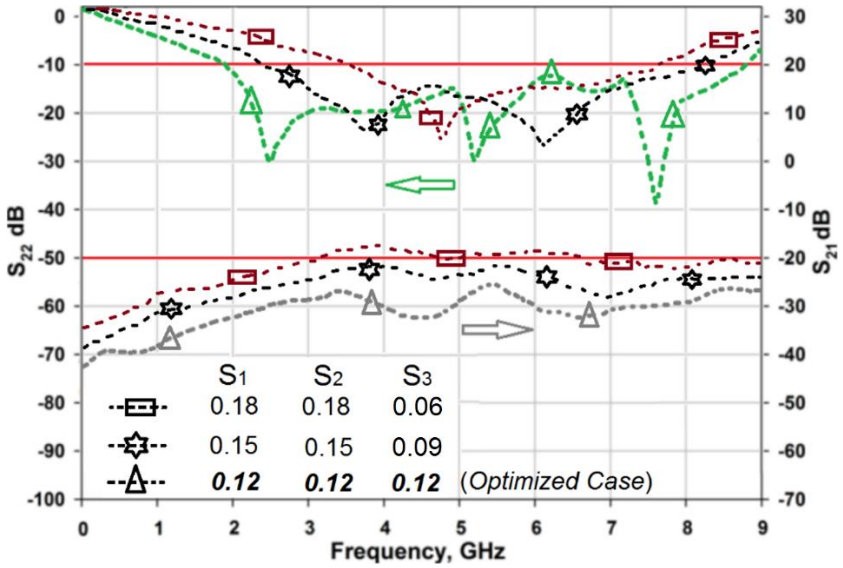


(b) 20 Ω (Dimensions of $S_1$, $S_2$, and $S_3$ are in millimeters)

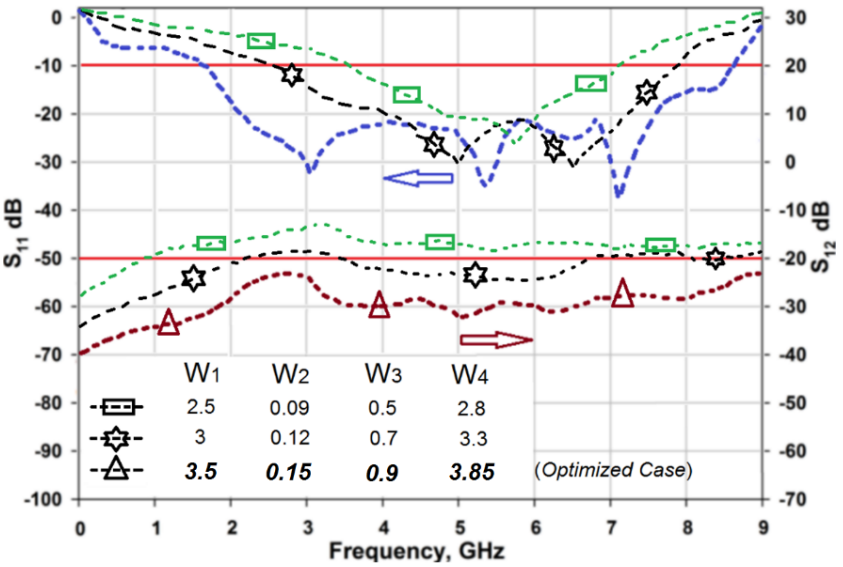


(c) 75 Ω (Dimensions of $W_1$, $W_2$, $W_3$ and $W_4$ are in millimeters)

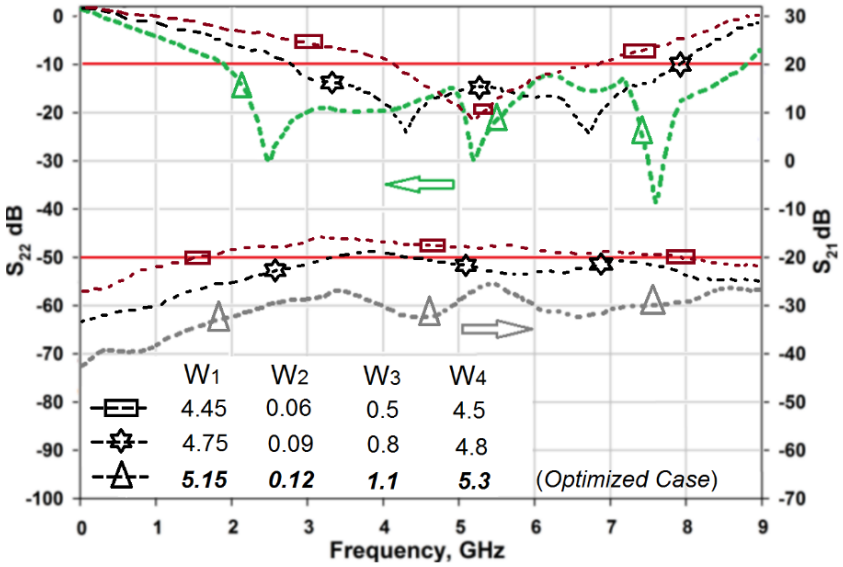


(d) 20 Ω (Dimensions of $W_1$, $W_2$, $W_3$ and $W_4$ are in millimeters)

Fig. 4. Transmission and reflection-coefficient response of the proposed MTM-TLs implemented using (a) 75 Ω, and (b) 20 Ω, accompanying the parametric studies on the key parameters.

Table IV. Effect of 75 Ω and 20 Ω CRLH MTM-TL on the Antenna's Performance. Other parameters given in Table III are fixed.

75 Ω CRLH MTM-TL

| *Key Parameters* (mm) | $S_{11} \leq$ -10 dB | $S_{12}$ | *Number of Resonance Frequency* |
|---|---|---|---|
| $S_1$:0.18, $S_2$:0.18, $S_3$:0.06 | 2.6 – 7.7 GHz | -20 dB at 5 GHz | one |
| $S_1$:0.15, $S_2$:0.15, $S_3$:0.09 | 2.2 – 8.25 GHz | -26 dB at 5 GHz | two |
| **$S_1$:0.12, $S_2$:0.12, $S_3$:0.12** | **1.7 – 8.65 GHz** | **-33 dB at 5 GHz** | **three (optimized case)** |

75 Ω CRLH MTM-TL

| *Key Parameters* (mm) | $S_{11} \leq$ -10 dB | $S_{12}$ | *Number of Resonance Frequency* |
|---|---|---|---|
| $W_1$:2.5, $W_2$:0.09, $W_3$:0.5, $W_4$:2.8 | 3.5 – 7.15 GHz | -17 dB at 5 GHz | one |
| $W_1$:3, $W_2$:0.12, $W_3$:0.7, $W_4$:3.3 | 2.6 – 7.9 GHz | -23 dB at 5 GHz | two |
| **$W_1$:3.5, $W_2$:0.15, $W_3$:0.9, $W_4$:3.85** | **1.7 – 8.65 GHz** | **-32 dB at 5 GHz** | **three (optimized case)** |

20 Ω CRLH MTM-TL

| *Key Parameters* (mm) | $S_{22} \leq$ -10 dB | $S_{21}$ | *Number of Resonance Frequency* |
|---|---|---|---|
| $S_1$:0.18, $S_2$:0.18, $S_3$:0.06 | 3.65 – 7.75 GHz | -20 dB at 5 GHz | one |
| $S_1$:0.15, $S_2$:0.15, $S_3$:0.09 | 2.3 – 8.3 GHz | -24 dB at 5 GHz | two |
| **$S_1$:0.12, $S_2$:0.12, $S_3$:0.12** | **1.85 – 8.8 GHz** | **-30 dB at 5 GHz** | **three (optimized case)** |

20 Ω CRLH MTM-TL

| *Key Parameters* (mm) | $S_{22} \leq$ -10 dB | $S_{21}$ | *Number of Resonance Frequency* |
|---|---|---|---|
| $W_1$:4.45, $W_2$:0.06, $W_3$:0.5, $W_4$:4.3 | 4.15 – 7.9 GHz | -17 dB at 5 GHz | one |
| $W_1$:4.75, $W_2$:0.09, $W_3$:0.8, $W_4$:4.8 | 2.8 – 8.0 GHz | -23 dB at 5 GHz | two |
| **$W_1$:5.15, $W_2$:0.12, $W_3$:1.1, $W_4$:5.3** | **1.85 – 8.8 GHz** | **-30 dB at 5 GHz** | **three (optimized case)** |

*B. Travelling-Wave Antenna Design*

The proposed CRLH MTM-TL antenna provides a guiding structure for a travelling wave as the main radiating mechanism. Here the surface currents that generates the RF signal travels through the antenna in one direction from port 1 to a terminated port 2, which is contrary to conventional standing wave or resonant antenna, such as the monopole or dipole, where RF signal travels in both directions reflected between the ends of the antenna. The length of the branch-line couplers arms are less than one quarter guide-wavelength. The results presented below show that the proposed travelling

wave antenna, which is a non-resonant structure, exhibits a wider operational bandwidth. The travelling-wave antenna is implemented using CRLH-MTM transmission-lines on a 0.8 mm thick Rogers RO4003 substrate. It is designed to operate over 1.8–8.4 GHz and 2–8.6 GHz using 75 Ω and 20 Ω MTM-TLs. The layout of the travelling-wave antenna is shown in Fig. 5, where $a \times b$ = 21.5×30 mm$^2$. The proposed antenna has the features of easy fabrication, low profile and low cost. The structure was built and its performance characterized using Agilent 8722ES vector network analyzer.

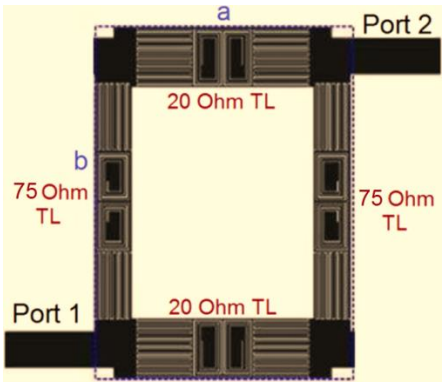


Fig. 5. Layout of the proposed CRLH MTM-TL travelling wave antenna.

The simulated and measured S-parameters of the proposed TWA are shown in Fig. 6. The measured and simulated results agree well with each other. At the measured center frequency of 5.2 GHz, the return-loss of the TWA between ports 1 and 2 is better than -32 dB, and the isolation is better than -22 dB over its operating bandwidth. Table V shows the proposed TWA structure provides a large fractional bandwidth exceeding 124%.

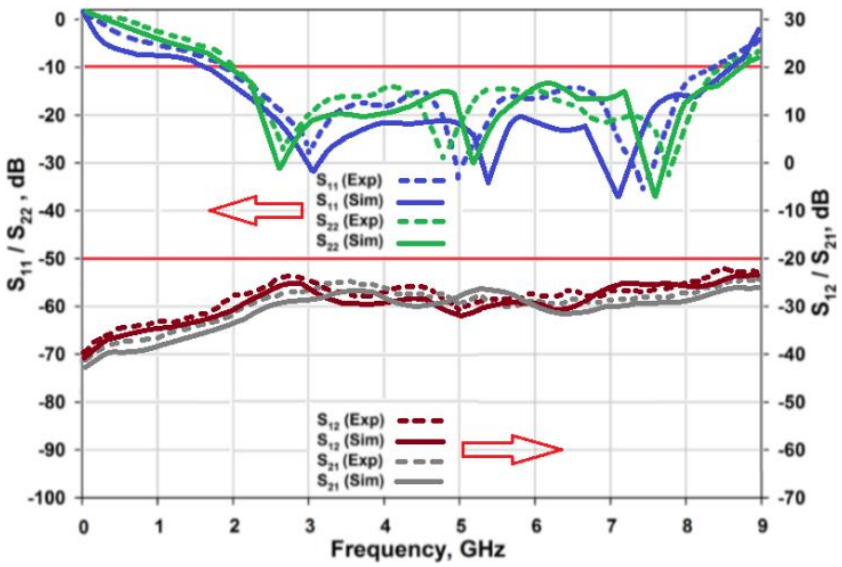


Fig. 6. Simulated and measured transmission and reflection-coefficient response of the proposed CRLH MTM-TL TWA.

Table V. Fractional Bandwidth of the Proposed TWA

| | |
|---|---|
| Measured ($S_{11}$) | 1.80 – 8.40 GHz ≈ 129.41% |
| Simulated ($S_{11}$) | 1.60 – 8.65 GHz ≈ 137.56% |
| Measured ($S_{22}$) | 2 – 8.60 GHz ≈ 124.52% |
| Simulated ($S_{22}$) | 1.85 – 8.75 GHz ≈ 130.18% |

Fig. 7 shows the photograph of the proposed travelling-wave antenna. The dimensions of the CRLH MTM-TL TWA are 21.5×30.0 mm$^2$ or $0.372\lambda_0 \times 0.520\lambda_0$ at 5.2 GHz (center frequency). The resulting TWA using CRLH MTM-TL

is compact compared to traditional TWA designed at the same frequency using quarter-wavelength transmission-lines of length ~51 mm. The other advantage of the proposed design is it does not use lumped elements, via-holes or defected ground structures that can complicate the fabrication process and therefore inflate the cost of the TWA.

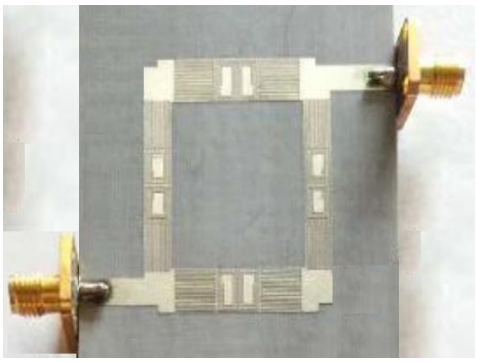

Fig. 7. Photograph of the fabricated CRLH MTM-TL TWA.

The simulated and measured gain and efficiency response of the CRLH MTM-TL TWA are shown in Fig. 8. The antenna's simulated and measured peak gain and efficiency at 5.5 GHz are 4.5 dBi and 88%, and 4.2 dBi and 81%, respectively. The figure also shows the effect of inter-digital capacitor ($L_1$), dual-spiral inductive slot elements ($L_2$), and the gap ($L_3$). Clearly, by increasing these lengths the antenna's effective aperture is increased, consequently the antenna's gain and radiation efficiency are enhanced over its operating frequency bandwidth. The gain and radiation efficiency of the antenna are tabulated in Table VI.

A standard anechoic chamber, shown in Fig. 9 was used to measure the antenna gain. It consists of a transmitting horn antenna located at the focal point of the reflector, which converted the spherical waves to plane waves toward the antenna under test (AUT). The antenna gain was measured using the standard comparative method. Connector losses were considered in the measurement. As well as, the antenna's radiation efficiency was calculated by taking the ratio of the radiated power to the input power of the antenna. The agreement between the simulated and measured results is generally good, and the discrepancy in the results is attributed to tolerance in the manufacturing of the antenna.

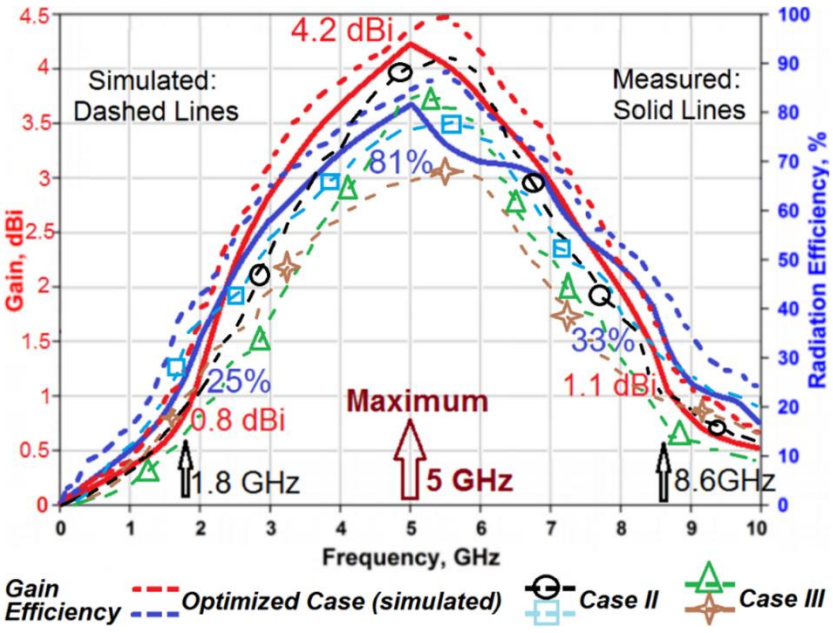

| 75 Ω CRLH MTM-TL | $L_1$ | $L_2$ | $L_3$ |
|---|---|---|---|
| **Case I (optimized) (mm)** | **6.5** | **1.4** | **9.8** |
| Case II (mm) | 5.5 | 1 | 8.6 |
| Case III (mm) | 4.5 | 0.6 | 7.4 |

| 20 Ω CRLH MTM-TL | $L_1$ | $L_2$ | $L_3$ |
|---|---|---|---|
| **Case I (optimized) (mm)** | **5.95** | **1.4** | **6.1** |
| Case II (mm) | 4.95 | 1 | 4.9 |
| Case III (mm) | 3.95 | 0.6 | 3.7 |

Fig. 8. Simulated and measured gain and radiation efficiency response of the TWA as a function of $L_1$, $L_2$, and $L_3$. Other parameters are kept constant and given in Table III.

Table VI. Simulated and Measured Gain and Radiation Efficiency of the Proposed TWA

| Frequency (GHz) | 1.8 | 2 | 3 | 5 | 6 | 7.4 | 8.4 | 8.6 |
|---|---|---|---|---|---|---|---|---|
| Simulated gain (dBi) | 1.1 | 1.55 | 3.1 | 4.35 | 4.15 | 2.8 | 1.75 | 1.45 |
| Measured gain (dBi) | 0.8 | 1.2 | 2.8 | 4.2 | 3.7 | 2.5 | 1.4 | 1.1 |
| Simulated efficiency (%) | 35 | 42 | 66 | 84 | 78 | 61 | 46 | 38 |
| Measured efficiency (%) | 25 | 33 | 58 | 81 | 70 | 55 | 41 | 33 |

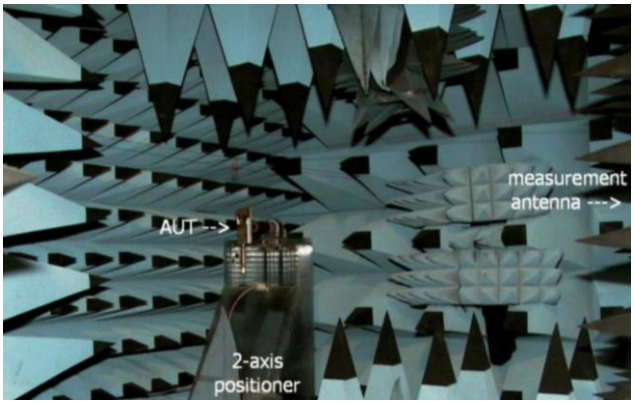

Fig. 9. Standard anechoic chamber used to measure the antenna's characteristics.

The measured E-plane and H-plane radiation patterns of the proposed TWA at spot frequencies in its operating band are plotted in Figs. 10 and 11, respectively. The radiation patterns were measured in an anechoic chamber. The co-polarization and cross-polarization radiation patterns of the TWA in both E-plane and H-plane at 1.8 GHz, 5 GHz, and 8.6 GHz are shown in Figs. 10 and 11. In the E-plane it radiates bidirectionally, and in the H-plane it radiates omni-directionally. The radiation is stable over its operating frequency range however its gain in the H-plane deteriorates at lower frequencies, which is attributed to weaker coupling through the series inter-digital capacitors.

Compared to similar branch-line geometries reported in [18], [22] and [23], the proposed antenna (i) operates over a much larger bandwidth (1.8–8.6 GHz); (ii) radiates omnidirectionally in the H-plane; (iii) has a peak gain and radiation efficiency of 4.2 dBi and 81%, respectively, at 5 GHz; (iv) and has dimensions of 21.5×30.0 mm$^2$. In contrast, the narrowband antenna reported in [22] radiates predominately unidirectionally, however it has a maximum gain of 6.6 dBi at 920 MHz (UHF) and 7.9 dBi at 2.45 GHz. The total size of this antenna is approximately 50×55 mm$^2$. The structure reported in [18] operates across over a limited frequency range between 0.99–1.01 GHz, and has dimensions of antenna of 28.4×39.75 mm$^2$. The structure recently reported in [23] operates at 0.93 GHz, and has dimensions of antenna of 52×56 mm$^2$.

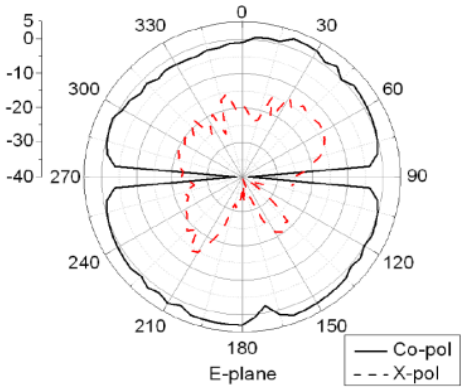


(a) 1.8 GHz

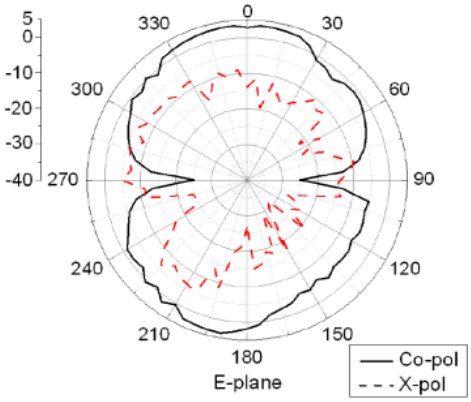


(b) 5 GHz

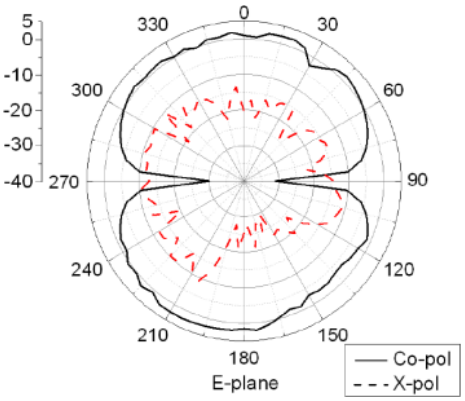


(c) 8.6 GHz

Fig. 10. Measured radiation patterns of proposed antenna in E-plane at: (a) 1.8 GHz, (b) 5 GHz, and (c) 8.6 GHz.

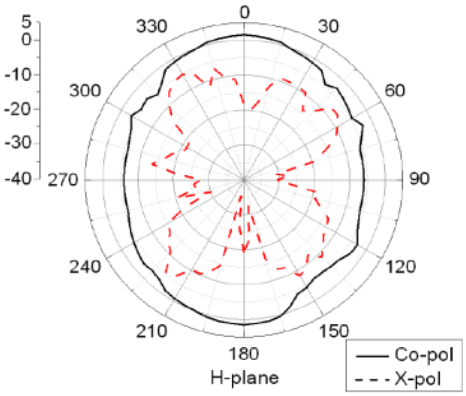


(a) 1.8 GHz

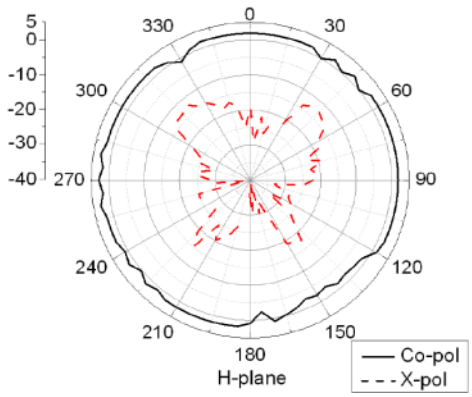


(b) 5 GHz

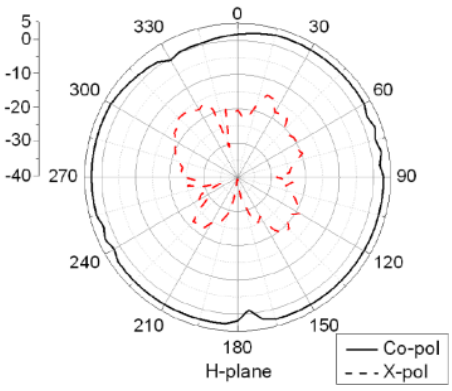


(c) 8.6 GHz

Fig. 11. Measured radiation patterns of proposed antenna in the H-plane at: (a) 1.8 GHz, (b) 5 GHz, and (c) 8.6 GHz.

## IV. CONCLUSIONS

The feasibility of a single-layer travelling-wave antenna design is demonstrated. The antenna design is based on metamaterial transmission-line implemented using inter-digital capacitors and embedded dual-spiral slot. The CRLH MTM-TLs used in the TWA design were implemented on 75 Ω and 20 Ω microstrip-lines. The proposed TWA avoids the use of lumped components, via-holes or defected ground structures hence making the TWA easy to fabricate at low cost. In addition, the low profile and planar CRLH MTM-TL TWA can be easily integrated into wireless communication systems. The dimensions of the proposed TWA are $21.5\times30.0$ mm$^2$ or $0.372\lambda_0\times0.520\lambda_0$, where $\lambda_0$ is free-space wavelength at 5.2 GHz, respectively. The TWA operates over an ultra-wideband (1.8 – 8.6 GHz) with a fractional bandwidth greater than 120%, and peak gain and efficiency of 4.2 dBi and 81%, respectively, at 5 GHz.

## REFERENCES


[1] D. M. Pozar, Microwave Engineering, 3rd ed., Wiley, New York, 2005.

[2] W.-S. Chang, and C.-Y. Chang, 'A high slow-wave factor microstrip structure with simple design formulas and its application to microwave circuit design,' IEEE Transactions on Microw. Theory & Tech., vol. 60, 2012, pp. 3376–3383.

[3] M. Alibakhshi-Kenari, M. Naser-Moghadasi, R. A. Sadeghzadeh, B. S. Virdee, and E. Limiti, "Periodic Array of Complementary Artificial Magnetic Conductor Metamaterials-Based Multiband Antennas for Broadband Wireless Transceivers" IET Microwaves, Antennas & Propagation, vol. 10, issue 15, Dec. 2016, pp. 1682–1691.

[4] M. Alibakhshi-Kenari, M. Naser-Moghadasi, R. A. Sadeghzadeh, B. S. Virdee, and E. Limiti, "New CRLH-Based Planar Slotted Antennas with Helical Inductors for Wireless Communication Systems, RF-Circuits and Microwave Devices at UHF-SHF Bands", Wireless Personal Communications- Springer Journal, Wireless Personal Communications, vol. 92, issue 3, Feb. 2017, pp. 1029–1038.

[5] M. Alibakhshi-Kenari, M. Naser-Moghadasi, R. A. Sadeghzadeh, B. S. Virdee, and E. Limiti, "Traveling-Wave Antenna Based on Metamaterial Transmission Line Structure for Use in Multiple Wireless Communication Applications", AEUE Elsevier-International Journal of Electronics and Communications, vol. 70, issue 12, Dec. 2016, pp. 1645–1650.

[6] S. R. Best, 'The significance of composite right/left-handed (CRLH) transmission-line theory and reactive loading in the design of small antennas,' IEEE Antennas and Propagation Magazine, vol. 56, no. 4, 2014, pp. 15–33.

[7] M. Alibakhshi-Kenari, M. Naser-Moghadasi, and R. A. Sadeghzadeh, 'Composite right−left-handed-based antenna with wide applications in very-high frequency−ultra-high frequency bands for radio transceivers,' IET Microwaves, Antennas & Propagation, vol. 9, no. 15, Dec. 2015, p. 1713 – 1726.

[8] H. Lee, J. H. Choi, C.-T. M. Wu, and T. Itoh, 'A compact single radiator CRLH-inspired circularly polarized leaky-wave antenna based on substrate-integrated waveguide,' IEEE Trans. on Antennas and Propagation, vol. 63, no. 10, Oct. 2015, pp. 4566–4572.

[9] C. Caloz, 'Metamaterial dispersion engineering concepts and applications,' Proc. of the IEEE, vol. 99, no. 10, 2011, pp. 1711–1719.

[10] M. Alibakhshi-Kenari and M. Naser-Moghadasi, 'Novel UWB miniaturized integrated antenna based on CRLH metamaterial transmission lines,' AEUE Elsevier, Int. Journal of Electronics and Communications, vol. 69, issue 8, Aug. 2015, pp. 1143–1149.

[11] C. Caloz and T. Itoh: Electromagnetic Metamaterials, Transmission Line Theory and Microwave Applications, Wiley and IEEE Press, 2005.

[12] N. Engheta, and R.W. Ziolkowski: Metamaterials: Physics and Engineering Explorations, New York: Wiley, 2006.

[13] R. Ahmed, A. Raslan, A. Ibrahim, and M. E. Safwat, 'Resonant-type antennas loaded with CRLH unit cell,' IEEE Antennas Wireless Propag. Lett., vol.12, 2013, pp. 23–26.

[14] C. J. Lee, K. M. K. H. Leong, and T. Itoh, 'Composite right/left-handed transmission line based compact resonant antennas for RF module integration,' IEEE Trans. Ant. and Propag., vol. 54, no. 8, 2006, pp. 2283–2291.

[15] M. Alibakhshi-Kenari, M. Naser-Moghadasi and R. A. Sadeghzadah, "The Resonating MTM Based Miniaturized Antennas for Wide-band RF-Microwave Systems" Microwave and Optical Technology Letters, Volume 57, Issue 10, pages 2339–2344, October 2015.

[16] M. Alibakhshi-Kenari, M. Naser-Moghadasi, R. A. Sadeghzadeh, B. S. Virdee, and E. Limiti, "New Compact Antenna Based on Simplified CRLH-TL for UWB Wireless Communication Systems", International Journal of RF and Microwave Computer-Aided Engineering, vol. 26, issue 3, March 2016, pp. 217–225.

[17] M. Gil, J. Bonache, J. Garcia-Garcia, et al., 'New left handed microstrip lines with complementary split rings resonators (CSRRs) etched in the signal strip,' IEEE MTT-S International Microwave Symposium Digest, 1419–1422, 2007.

[18] J. Zhang, J. Tao, B.-F. Zong, and C. Zhou, 'Compact branch-line coupler using uniplanar spiral based CRLH-TL,' Progress in Electromagnetics Research Letters, vol. 52, 2015, pp. 113–119.

[19] Y.-D. Yong, and T. Itoh, 'Metamaterial-based antennas,' Proceedings of the IEEE, vol. 100, no. 7, 2012, pp. 2271–2285.

[20] H-X. Xu, G.-M. Wang, C.-X. Zhang, "Compact design of branch-line coupler based on CRLH TL combined with fractal shaped geometry," International Conference on Microwave and Millimeter Wave Technology, 2010, pp. 1658–1661.

[21] S. Otto, A. Rennings, T. Liebig, C. Caloz, K. Solbach, 'An energy-based circuit parameter extraction method for CRLH leaky wave antennas,' IEEE Proceedings of the Fourth European Conference on Antennas and Propagation, April 2010, pp. 1–5.

[22] Y.-K. Jung, B. Lee, 'Dual-band circularly polarized microstrip RFID reader antenna using metamaterial branch-line coupler,' IEEE Trans. on Antennas and Propagation, vol. 60, no. 2, Feb. 2012, pp. 786–791.

[23] Q. Wang. J. Lim, Y. Jeong, 'Design of a compact dual-band branch line coupler using composite right/left-handed transmission lines,' Electronics Letters, April 2016, vol. 52, no. 8 pp. 630–631.